

## High-Resolution X-Ray-Photoemission Spectra of PbS, PbSe, and PbTe Valence Bands\*

F. R. McFeely, S. Kowalczyk, L. Ley,<sup>†</sup> R. A. Pollak,<sup>‡</sup> and D. A. Shirley

*Department of Chemistry and Lawrence Berkeley Laboratory, University of California, Berkeley, California 94720*

(Received 16 November 1972)

High-resolution x-ray-photoemission valence-band spectra (0–45 eV binding energy) of cleaved single-crystal PbS, PbSe, and PbTe are reported. The spectra are compared with available band-theory results. Relativistic orthogonalized-plane-wave results exhibit the best over-all agreement with experiment. Empirical-pseudopotential-method (EPM) results show similar agreement for all but the most tightly bound valence band. The uppermost peak, corresponding to the three least tightly bound bands, shows detailed structure in good agreement with the EPM predictions. The PbTe valence-band spectrum can be synthesized from the x-ray-photoemission valence-band spectra of Pb and Te.

### I. INTRODUCTION

The “lead salts,” PbS, PbSe, and PbTe, have in recent years been the object of considerable experimental and theoretical study, due in part to the technological importance of these materials as infrared and visible radiation detectors and in part to interest in their fundamental properties. All three salts crystallize in the rocksalt structure, which consists of two interlocking fcc lattices separated by a translation of  $(\frac{1}{2}a, \frac{1}{2}a, \frac{1}{2}a)$ , where the lattice constant  $a$  at 300 °K is 5.9362 Å for PbS,<sup>1</sup> 6.1243 Å for PbSe,<sup>2</sup> and 6.4603 Å for PbTe.<sup>3</sup> In this work, x-ray-photoemission spectroscopy (XPS) has been used to determine the valence-band density of states for each of the lead salts. Derived quantities are compared with several theoretical band-structure calculations, which are critically examined in light of these results.

Experimental procedures are described in Sec. II. Results are given in Sec. III and compared with theory in Sec. IV.

### II. EXPERIMENTAL

The samples used for these experiments were high-purity single crystals. In order to minimize contamination of the samples by adsorption of hydrocarbons and/or oxygen, the crystals were cleaved under dry nitrogen in a glove bag and placed in a Hewlett-Packard 5950 electron spectrometer at  $5 \times 10^{-9}$  Torr without exposure to the atmosphere. They were then irradiated with monochromatized Al  $K\alpha_{1,2}$  radiation (1486.6 eV), and the ejected photoelectrons were energy analyzed.

In addition to the valence-band region, spectra were taken over a binding energy range of 0–1000 eV in order to detect core-level peaks from any impurities which might be present. Experience has shown that even small amounts of impurities can give rise to extraneous peaks in the valence-band region. The only impurities present in detectable quantities were carbon and oxygen, and they were present in sufficiently small amounts so

as to preclude any serious effects on the valence-band spectra. The area ratios of the Pb  $4f_{7/2}$  line to the oxygen 1s line before and after the scan of each Pb-salt valence band (VB) are given in Table I. Furthermore, the symmetric shape of the Pb core levels indicate that the oxygen present was in adsorbed molecules on the surface of the sample rather than as oxide. This is further verified by the fact that the intensity of the O 1s line decreased when the crystal was left in vacuum overnight.

Energy conservation gives the photoemission equation

$$h\nu = E_B + E_K + q\phi_{sp},$$

where  $E_K$  is the kinetic energy of the photoelectron,  $\phi_{sp}$  is the work function of the spectrometer, and  $E_B$  is the binding energy with respect to the Fermi energy. This equation presumes that the emitting region of the crystal is electrically grounded to the spectrometer. If this were not the case, it would be necessary to include an extra additive term to account for charging. Our experience has shown that small-band-gap semiconductors, such as the lead salts, show little or no charging.

The Fermi level of the Pb salts with respect to that of the spectrometer was determined with a Au reference as follows. A small quantity of Au was evaporated onto the surface of each Pb salt after the valence-band measurement, and the Au  $4f_{7/2}$  line position was determined with respect to a core level in each case. The measured binding energy for gold metal of the Au  $4f_{7/2}$  level with respect to the Au Fermi energy is  $84.00 \pm 0.01$  eV. Thus the binding energy of the Pb-salt core level with respect to the Au Fermi level is  $84.00 \pm 0.01$  eV mi-

TABLE I. Ratio of Pb  $4f_{7/2}$  to O 1s peak areas.

	PbS	PbSe	PbTe
Before VB run	30 : 1	> 50 : 1	10 : 1
After VB run	44 : 1	> 50 : 1	33 : 1

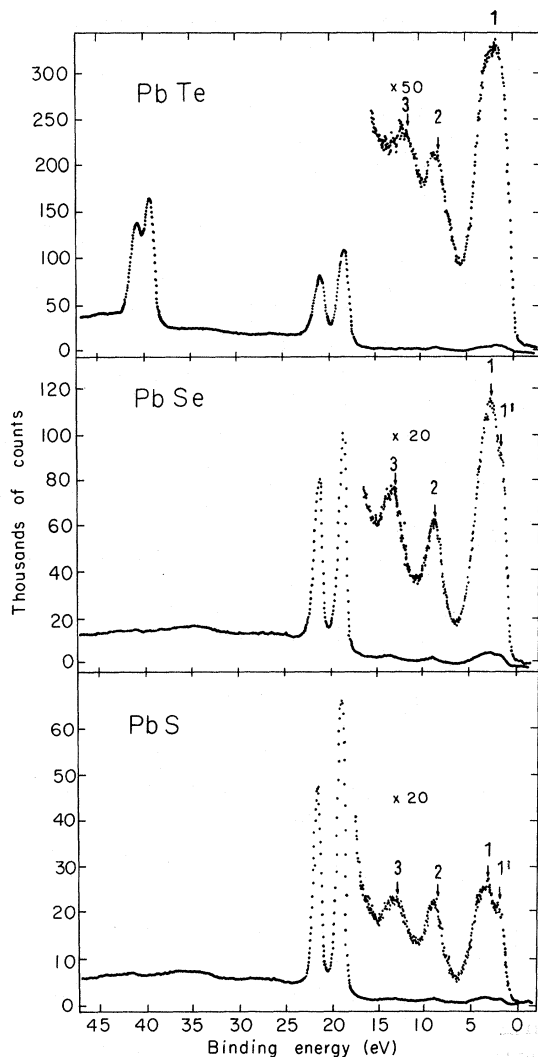


FIG. 1. Raw valence-band spectra of the lead salts; the strong double peaks at  $\sim 20$  eV are the lead  $5d_{3/2}$  and  $5d_{5/2}$  levels; the tellurium  $4d$  are at about 40-eV binding energy.

mus its separation from the Au  $4f_{7/2}$  peak. This binding energy then defines the Fermi level for the Pb-salt valence-band spectrum which includes the Pb-salt core level. All binding energies quoted in this paper are given with respect to this reference energy. It is assumed that the Fermi level of the deposited Au is equal to the Fermi level of the emitting portion of the sample.

### III. RESULTS

The spectra  $I(E)$  for each of the three lead salts are shown in Fig. 1. There is striking similarity in the valence-band spectra of the three salts. The positions of the corelike Pb  $5d_{5/2}$  peaks for these salts vary within a range of 0.2 eV and the values of the spin-orbit splitting in the Pb  $5d$  peaks are identical to within experimental error (0.02 eV). The spectra show in each case a strong broad peak, which we call peak 1, centered at about 2–2.5 eV below  $E_F$ , and exhibiting quite prominent structure on the low-binding-energy side. This structure is evident only as a shoulder in PbTe, but in progressing through PbSe to PbS it becomes a well-defined extra peak which we label 1'. Between the 1-1' peak and the Pb  $5d$  lines there are two less intense peaks labeled 2 and 3 in Fig. 1. The absolute binding energies of these peaks show no monotonic trend with the atomic number of the group-VI element. Peaks 2 and 3 have the highest binding energies in PbSe. However, the energy difference between peaks 2 and 3 increases monotonically in going from the telluride to the sulfide. The 3-2 splitting is 3.5 eV in the telluride, 4.3 eV in the selenide, and 4.4 eV in the sulfide. The experimental binding energies are given in Table II.

### IV. DISCUSSION

These group-IV-VI compounds have a total of ten valence electrons per Pb atom, which must occupy five valence bands. In light of many recent band-structure calculations, the 1-1' peak structure of the photoelectron spectra in all three lead salts may be unequivocally identified with three  $p$ -like bands. At the  $\Gamma$  point, two of these bands are degenerate and have  $\Gamma_3^-$  symmetry, while the third band has  $\Gamma_5^-$  symmetry. Calculations of the band structure by the empirical-pseudopotential-method<sup>4-6</sup> (EPM), the orthogonalized-plane-wave-method,<sup>7</sup> and the relativistic augmented-plane-wave<sup>8,9</sup> (APW) method give qualitative agreement on this point.

While there is reasonable agreement on the positions of the three  $p$ -like bands and the corresponding maxima in the densities of states, agreement among theoretical predictions of the two lower-lying peaks, 2 and 3, is much poorer. Clearly these peaks can only represent the two  $s$ -like ( $\Gamma_6^+$ )

TABLE II. Pb-salt valence-band binding energies (eV).

	Pb $5d_{3/2}$	Pb $5d_{5/2}$	3	2	1	1'
PbTe	$20.94 \pm 0.05^a$	$18.33 \pm 0.05$	$11.7 \pm 0.2$	$8.20 \pm 0.1$	$2.30 \pm 0.1$	...
PbSe	$20.99 \pm 0.05$	$18.38 \pm 0.05$	$12.92 \pm 0.15$	$8.64 \pm 0.1$	$2.19 \pm 0.1$	$1.21 \pm 0.15$
PbS	$21.10 \pm 0.05$	$18.52 \pm 0.05$	$12.81 \pm 0.15$	$8.43 \pm 0.1$	$2.53 \pm 0.1$	$1.20 \pm 0.1$

<sup>a</sup>The quoted errors do not include uncertainties in the determination of the Fermi level.

bands arising from the 6s level of Pb and the highest s level of the group-VI atom. Neither peak can be due to impurities since, as stated previously, no core-level peaks were observed for any element which would contribute significant intensity to the valence-band region. Nor can peak 3 be an energy-loss peak arising from the 1-1' peak; first, because the energy difference of ~10 eV is too small compared to the ~16-eV loss structure observed for the Pb 5d electrons in these salts, and second, because the intensity of peak 1-1' relative to peak 3 is far lower than the corresponding ratio of the Pb 5d peak to its energy-loss structure. The assignment of the spectra therefore appears to be completely straightforward. The peak 1-1' complex arises from the top three "p-like" bands and peaks 2 and 3 each arise from an "s-like" band.

Band-structure experiments and theory enjoy a symbiotic relationship. This relation is valuable because neither would be very effective alone. However, the closeness of the two requires that in the interpretation of spectra, one should clearly differentiate between results that are derived directly from the spectra and results that are inferred by comparing the spectra with calculated band structures. We have already identified the peaks in the lead-salts spectra with energy bands, so some interplay of theory and experiment has already taken place. In fact, these peaks are sufficiently well resolved that they could have been assigned to the energy levels of the pure elements without reference to band structure, as we shall show below. We assume throughout this discussion that the one-electron-transition model described by Fadley and Shirley<sup>10</sup> can be used for the Pb salts. We also assume that calculated eigenvalue spectra of band theory represent experimental one-electron binding-energy spectra (Koopmans's theorem).<sup>11</sup> It should be emphasized at this point that disagreement between theory and experiment may result from the inapplicability of either of these assumptions.<sup>10,11</sup> Turning now to a more detailed interpretation of the spectra within this model, we can proceed at two distinct levels of sophistication.

*Level 1.* The mean peak positions and widths can be extracted directly from the spectra and used to assess the relative accuracies of the band-structure calculations. This is an empirical approach, and therefore less subject to error, but it yields information only about the gross features of the bands.

*Level 2.* After one or more band-structure calculations have been judged to be in good agreement with experiment, these energy bands can be compared in more detail with the shape or at least the width of the peaks to estimate the energies of the bands at symmetry points in the Brillouin zone. This procedure is somewhat speculative, but it

yields information of reasonable reliability about the really interesting features of the band structure.

In this discussion below we shall first discuss each of the available band-structure calculations at level 1, then go on to level 2.

Overhof and Rössler<sup>12</sup> calculated the band structures of all three Pb salts using a relativistic Green's-function technique. Their calculation is unique among those considered here in that the d electrons are included. Unfortunately, their band structures must be viewed in light of our results as being qualitatively wrong. The highest s level is predicted in all three cases to lie so close to the p-like bands as to give rise to only one broad peak in the density of states rather than one p peak and a smaller s peak ~6 eV away. Furthermore, the lower-lying s peak would in all three cases be buried under the corelike Pb 5d peaks. The Pb 5d<sub>3/2</sub> and 5d<sub>5/2</sub> are predicted to lie at ~13.5 and 15.5 eV for PbS, ~13.3 and 15.4 eV for PbSe, and ~13.6 and 15.5 eV for PbTe instead of the ~18.5–21 eV given for the three salts by our spectra. We have not corrected our XPS spectra for polarization or relaxation about the final-state hole, and thus the reported binding energies for the Pb 5d electrons—and to a lesser extent peaks 2 and 3—may be smaller than the Koopmans-theorem value of theory. This correction may consist of adding approximately 1 eV to the Pb 5d binding energies.

The APW method was used by Conklin, Johnson, and Pratt<sup>8</sup> to calculate the band structure of PbTe. The Hamiltonian used for this calculation included a spin-orbit term and Darwin and mass-velocity corrections. The results obtained agree reasonably well with our spectra. The calculation indicates that the highest s peak should occur near 6 eV, while the other s peak should be at 11 eV, compared with the experimental values 8.2 and 11.7 eV obtained here.

Augmented-plane-wave calculations very similar to those above were undertaken by Rabii<sup>9</sup> on PbS and PbSe. The upper  $\Gamma_6^+$  levels were calculated, and it appears that they would lead to maxima in the density of states around 7 eV in both PbSe and PbS, with the peak probably lying slightly lower in energy for PbSe. This compares with experimental values for this peak of 8.6 and 8.4 eV, respectively. Thus the discrepancy is similar to that in the PbTe case.

A different approach to the problem was taken by Lin and Kleinman<sup>4</sup> in a pseudopotential calculation of the lead-salt band structures. In this calculation there were five variable parameters which were adjusted to give the best agreement with reflectivity data.<sup>13</sup> The charge of Pb and the group-VI atom were allowed to vary, and there was also

TABLE III. Calculations of Lin and Kleinman (LK) (Ref. 4) compared to experiment.

	PbS		PbSe		PbTe	
	LK	Expt.	LK	Expt.	LK	Expt.
Peak 1	1.8	2.5	1.7	2.2	2.5	2.3
Peak 2	6.3	8.4	5.8	8.6	5.4	8.2
Peak 3	12.2	12.8	11.8	12.9	8.7	11.7

TABLE IV. Calculations of Herman *et al.* (Ref. 7) compared to experiment.

	PbS		PbSe		PbTe	
	OPW	Expt.	OPW	Expt.	OPW	Expt.
Peak 1	2.6	2.5	~2.6	2.2	~2.0	2.3
Peak 2	6.6	8.4	7.4	8.6	7.4	8.4
Peak 3	14.0	12.8	14.0	12.9	11.5	11.7

a spin-orbit parameter. The remaining two parameters were used to adjust an extra repulsive-potential term which applies only to *s*-like levels. The variation of these parameters ultimately produced shifts of up to 17.7 eV in PbS and 7.6 in PbTe. A comparison of the predictions of their band structures and experiment is given in Table III. As can be seen, the over-all agreement is quite good in PbS and PbSe, except that, as with the APW calculations, the predicted binding energy of peak 2 is too low. In the PbTe calculation, however, the agreement is poor for peak 3 as well.

Tung and Cohen<sup>5</sup> and Tsang and Cohen<sup>6</sup> have calculated the band structures for PbTe and for PbSe and PbS, respectively, using the EPM (see Figs. 2 and 3). In these calculations spin-orbit interaction was included but other relativistic effects were not. In addition to band structures, the resulting densities-of-states curves were calculated.

The results of these calculations, shown in Fig. 2, match the experimental results for the *p*-like peak(s). Particularly striking is the way in which the calculation shows the origin of the 1' peak out of the 1 peak in progressing from PbTe to PbS. The position indicated for the highest *s* band (not shown) is also reasonable though not exactly cor-

rect.

The major disagreement of this calculation with experiment lies in the predicted energy of the lowest *s* peak (not shown in the density-of-states curve). This level is predicted to lie at 17 eV in PbTe, 24.5 eV in PbSe, and 27.5 eV in PbS. This discrepancy is not unexpected, because a local pseudopotential was used. In the case of ZnSe,<sup>14</sup> a local pseudopotential was shown to be inadequate for the lowest bands. Thus the nonlocal nature of the pseudopotential should be considered when calculating these bands.

The most successful band-structure calculation was undertaken by Herman *et al.*<sup>7</sup> (see Fig. 4). In this calculation the OPW method, with relativistic effects included directly in the Hamiltonian, was used to calculate the energy levels at certain symmetry points in the Brillouin zone. A pseudopotential technique was then used to connect the regions between the symmetry points. The resulting band structures were not fitted to any experimental data. The results for PbTe, PbSe, and PbS are shown in Table IV. While the predicted binding energy for peak 2 in PbS and PbSe is lower than observed (as is the case in all the band structures), the results for PbTe agree very well with experiment.

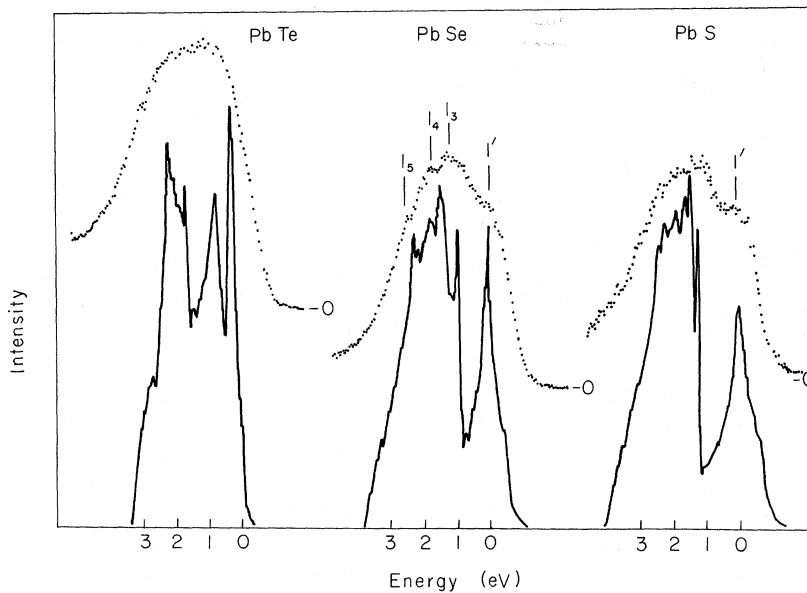


FIG. 2. EPM densities of states (Refs. 5 and 6) compared with the shape of the 1-1' peaks in the valence bands of the lead salts (relative energy scale).

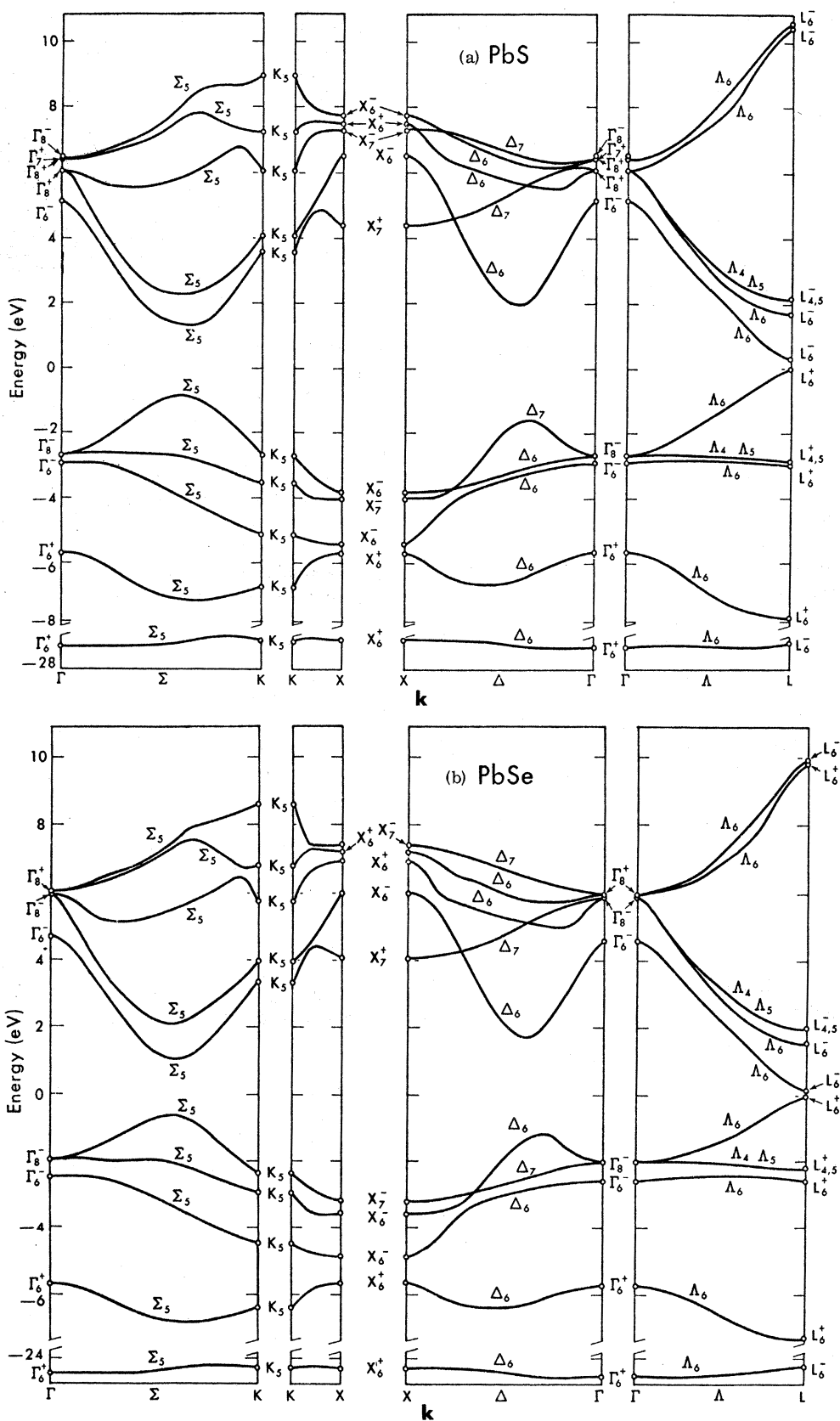


FIG. 3. (Continued)



have the maximum in the top band near  $\Delta$ , about 3.4 eV above the bottom of the third band (at  $X_6^+$ ), while the EPM value is 4.0 eV. It is difficult to obtain an experimental value for this quantity from the spectra, but a value of  $3.9 \pm 0.2$  can be estimated by assuming that the peak has a constant slope down to zero intensity, as indicated in the EPM  $\rho(E)$ .

In summary, our spectrum shows good agreement with the two theories regarding total width of the top band, giving  $5.2 \pm 0.3$  eV vs 5.5 eV (EPM) or 5.2 eV (OPW), but in detail there is some disagreement. The position of peak 1' appears to be higher than either theory would predict by  $\sim 0.2$ – $0.4$  eV. Peak 1' is closer to point 1'' than the EPM results (by  $\sim 0.4$  eV), and higher above the bottom of these bands than the OPW prediction (by  $\sim 0.6$  eV).

Peak 2 in PbS has its center 7.0 eV below 1', or about 8.2 eV below  $E_F$  and presumably also the top of the valence bands. The full width at half-maximum (FWHM) of this peak is 2.5 eV and the total width, based on an uncertain extrapolation to zero intensity, is about 3.5 eV. The centroid in the EPM  $\rho(E)$  is 7.1 eV below the top of the bands or 5.6 eV below 1'—about 1 eV or more too high. The width that should be compared to the experimental FWHM (in the absence of lifetime broadening) is about 1.2–1.4 eV (because of instrumental broadening), and the total bandwidth is about 2.1 eV; both are thus substantially narrower than experiment. The OPW extrema of this band are 5.8 and 8.1 eV below the top of the valence bands. Thus the OPW bandwidth of 2.3 eV is too small. We estimate that the OPW centroid in  $\rho(E)$  would lie about 7.3 eV below the top of the valence band, or about 0.9 eV too high. Use of point 1' as a fiducial point would worsen the agreement, since this point

is already too low in the OPW results. In summary, peak 2 is about 1 eV lower and  $\sim 50\%$  wider than predicted by the OPW and EPM theories. Of course, the observed binding energy may be affected by relaxation and the linewidth by lifetime broadening.

The centroid of peak 3 falls at 12.5 eV below  $E_F$ , or about 1.6 eV higher than the  $14.1 \pm 0.2$  eV that we can estimate as the distance that the bottom band falls below the top of the valence band in the OPW calculations. The peak width shows a larger discrepancy. The OPW band is only 0.7–0.8 eV wide, while peak 3 is about 2.6 eV FWHM or  $\sim 4$  eV in total width. Thus band-structure broadening may be more pronounced for this band than the calculations indicate.

Turning now to PbSe, there is a considerable amount of partially resolved structure in peak 1. The shoulder on the high-energy side (peak 1') is clearly discernible, although not quite as well resolved as in PbS. Peak 1' is  $1.16 \pm 0.10$  eV below  $E_F$ —in excellent agreement with the highest-energy maximum in the EPM  $\rho(E)$ , which is also less resolved from the rest of peak 1 and is centered 1.18 eV below the top of the valence bands.

The rest of peak 1 in PbSe is similar to the PbS case, but more structure is evident. The resolution of other features is marginal, but four more features could be reproducibly identified in three samples. They were 1'', an abrupt change of slope similar to 1'' in PbS; 1<sub>3</sub>, a peak connected to 1' by a gently sloping line; 1<sub>4</sub>, a peak separated from 1<sub>3</sub> by a distinct minimum; and 1<sub>5</sub>, another shoulder on the low-energy side of peak 1. The positions of the last four features relative to 1' are given, for all three samples, in Table V. Also given in Table V are the positions of the five most prominent peaks in the EPM  $\rho(E)$ . The agreement with ex-

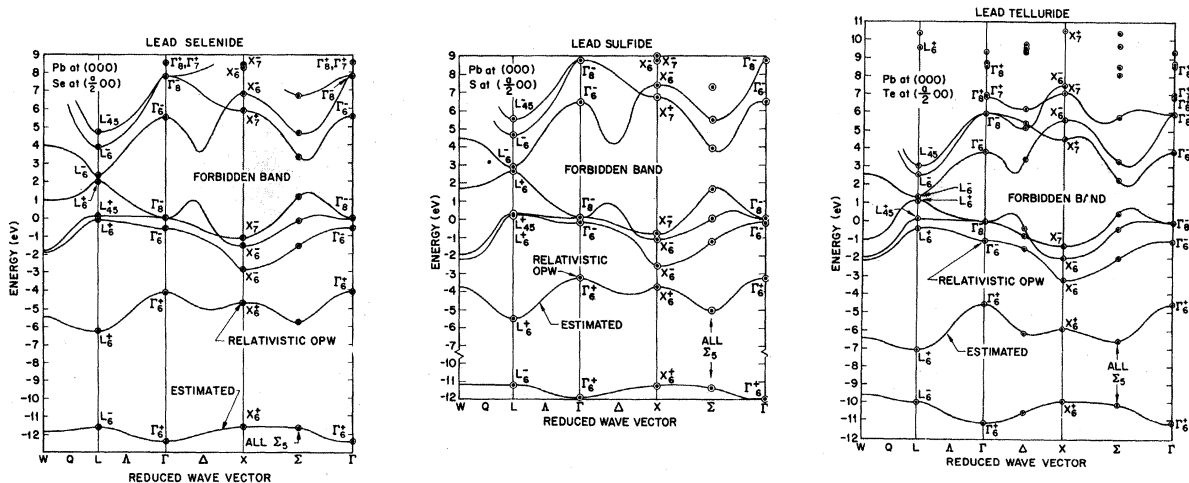


TABLE V. Features in peak 1 of PbSe (energies in eV).

Sample	1'	1''	1 <sub>3</sub>	1 <sub>4</sub>	1 <sub>5</sub>
I	(0)	0.7 <sup>a</sup>	1.0 <sub>5</sub>	1.5 <sub>5</sub>	2.2 <sub>5</sub>
II	(0)	0.7 <sub>1</sub>	1.2 <sub>5</sub>	1.7 <sub>5</sub>	2.4 <sub>8</sub>
III	(0)	0.6 <sub>5</sub>	1.1	1.6 <sub>5</sub>	2.3 <sub>5</sub>
Theory (EPM)	(0)	0.9	1.35	1.8	2.2

<sup>a</sup>These positions are known to  $\pm 0.1$  eV relative to one another.

periment is very good. Equally impressive (and more important) is the agreement between the general shapes of this peak in  $\rho(E)$  and  $I(E)$ . Again peak 1' is slightly closer to the rest of peak 1 and not as well resolved as the EPM results would suggest, but the over-all agreement is really extraordinary.

Further comparisons with the EPM  $\rho(E)$  give  $1' - 1_6 = 2.9$  eV (expt) and 2.7 eV (EPM) and  $1' - 1_7 \cong 4$  eV (expt) and 3.7 eV (EPM), where  $1_6$  is the position of half-maximum height on the low-energy side of peak 1, and  $1_7$  is the bottom of these bands, extrapolated from the slope. Again the agreement is excellent. The experimental  $I(E)$  and the EPM  $\rho(E)$  are plotted in Fig. 2.

No  $\rho(E)$  is available from the OPW calculations, but it is clear that the OPW and EPM results for peak 1 in PbSe agree very well, as point-by-point comparison of the energy bands will show. The OPW results give the maximum in the top band near  $\Delta$  as 1.1 eV below the top of the valence bands at  $L_6^*$ . If this may be taken as a measure of the position of 1', the agreement is excellent. The next two bands have flat regions along  $\Gamma$ - $L$ , at  $\sim 2.0$  and 2.4 eV below  $L_6^*$  (OPW), or 2.1 and 2.5 eV (EPM). These two bands probably contribute significantly to the features 1'' and 1<sub>3</sub> in  $I(E)$ , at  $\sim 1.85$  and 2.3 eV below  $E_F$ . It would be very plausible simply to interpret these features as determining the positions of  $L_{45}^*$  and  $L_8^*$ , but such an interpretation is not unique. Finally, the total width of these top three bands is 4.9 eV (OPW), in good agreement with 4.9 eV (EPM) and  $\approx 5$  eV (expt).

Peak 2 in PbSe shows no appreciable structure.

TABLE VI. Characteristic energies in Pb salts (eV).

Description	PbTe		PbSe		PbS	
	OPW <sup>a</sup>	EPM <sup>b</sup>	OPW <sup>a</sup>	EPM <sup>b</sup>	OPW <sup>a</sup>	EPM <sup>b</sup>
$L_6^*$	0	0	0	0	0	0
$\Delta_6$	0.7	0.6	1.1	1.1	1.8	1.6
$L_{4,5}^*$	1.0	0.9	1.9	2.2	2.3	2.8
$X_6^*$	4.3	3.7	4.9	4.9	5.2	5.5

<sup>a</sup>Taken from Refs. 5 and 6.

<sup>b</sup>Taken from Ref. 7.

TABLE VII. Comparison of PbTe results with those for Pb and Te. Binding energies are relative to the measured Fermi levels. All units are eV.

	PbTe	Pb <sup>a</sup>	Te <sup>b</sup>
Binding energy			
Te $4d_{3/2}$	40.95(7)	...	41.80(9)
Binding energy			
Te $4d_{5/2}$	39.49(7)	...	40.31(9)
FWHM $4d_{3/2} = \text{FWHM } 4d_{5/2}$	1.50(2)	...	0.94(2)
4d splitting	1.46(2)	...	1.51(1)
Binding energy			
Pb $5d_{3/2}$	20.94(7)	20.32(5)	...
Binding energy			
Pb $5d_{5/2}$	18.33(7)	17.70(5)	...
FWHM $5d_{3/2} = \text{FWHM } 5d_{5/2}$	1.20(5)	0.94(5)	...
5d splitting	2.61(2)	2.62(2)	...
Binding energy			
Te 5s, PbTe "3"	11.7(2)	...	11.5(2)
FWHM Te 5s, PbTe "3"	2.5(3)	...	4.8(5)
Binding energy			
Pb 6s, PbTe "2"	8.20(11)	7.68(20)	...
FWHM Pb 6s, PbTe "2"	2.3(2)	2.7(2)	...
Binding energy			
Pb 6p, Te 5p, PbTe "1"	2.30(11)	(2.33(8) 0.53(5))	(4.0(2) 1.13(5))
FWHM Pb 6p, Te 5p, PbTe "1"	3.5(2)	3.1(2)	5.0(2)

<sup>a</sup>Reference 15.

<sup>b</sup>Reference 16.

Its position at 7.1 eV below 1', or 8.3 eV below  $E_F$ , is about 1.5 lower than the corresponding peak in the EPM  $\rho(E)$  at 6.8 eV, and its width (FWHM = 1.8 eV) is about twice that of the EPM peak (FWHM = 0.9 eV). In the OPW results this band appears to be about the same width as in the EPM case, although comparison is difficult because  $X_6^*$  lies below  $\Gamma_6^*$  in OPW and above it in EPM. We estimate the centroid of this band to lie about 6.6 eV below 1' in the OPW case, in better agreement with experiment, but still slightly high.

Peak 3 in PbSe is centered 11.7 eV below 1' or 12.9 eV below  $E_F$ , about 1 eV higher than the lowest OPW band, which would give a peak at an estimated 12.8 eV below 1' or 13.9 eV below the top of the valence bands. Again the peak is wider (1.9 eV FWHM, or  $\approx 3.5$  eV total) than the OPW band (0.8 eV total), though not as wide as peak 3 in PbS.

In PbTe, peak 1 has a rather different structure from the same peak in PbS and PbSe. First, the shoulder attributed to peak 1' is not evident. This is in very good agreement with the EPM  $\rho(E)$ , which does not show the well-separated peak found in the other salts. This is a consequence of the general tendency for the top three bands to be compressed upward in PbTe relative to PbSe and PbS. Table VI contains the positions of several symmetry points relative to the top of the valence bands ( $L_6^*$ ) from the OPW and EPM calculations. The

compression of these bands in PbTe is especially pronounced for features near the top of the band.

Since there is no peak 1' in PbTe, another fiducial point is needed. We shall use the energy of the leading edge at half-height, denoted  $1_H$ . Its value is 17.99 eV above  $E(5d_{5/2})$ , or  $0.34 \pm 0.05$  eV below  $E_F$ . This agrees very well with the value  $0.4 \pm 0.1$  eV estimated from the EPM  $\rho(E)$  as the energy of this feature below the top of the valence bands (at  $L_6^+$ ). The error in this estimate follows from uncertainties in converting  $\rho(E)$  to  $I(E)$ .

Peak 1 in the PbTe  $I(E)$  can be characterized as "blunt." This agrees well with the EPM  $\rho(E)$  after due allowance for experimental resolution has been made. At slightly higher resolution considerably more structure should be discernible. The peak is somewhat wider than the theoretical results would indicate. The trailing edge at half-height falls at  $E_F - 3.84 \pm 0.2$  eV, compared with  $E_F - 3.2$  eV for this feature from the EPM  $\rho(E)$ . Rough extrapolation gives the total bandwidth as  $\sim 5$  eV, compared to 4.3 eV (OPW) and 3.7 eV (EPM).

The positions and widths of peaks 2 and 3 in PbTe are set out in Table VII. Peak 2 is about 1 eV lower than the OPW result and nearly 2 eV below the EPM value. The OPW peak positions for peak 3 is in very good agreement with experiment. Again both of these peaks are wider than the band-structure  $\rho(E)$  would predict.

We have identified the peaks in the XPS  $I(E)$  spectrum with peaks of corresponding energy in  $\rho(E)$  of band theory. The same assignments can be obtained empirically by comparing the XPS valence-band spectra of the lead salts with those of the pure elements comprising them. For example, there is a 1-to-1 relationship between the peaks in  $I(E)$  of PbTe and the sum of peaks in the  $I(E)$  spectra of single-crystal Pb<sup>15</sup> and single-crystal Te.<sup>16</sup> The binding energies of these peaks are listed in Table VII. It can be seen that the difference between any two corresponding peaks, one from the salt and one from the element, is at most  $\sim 0.6$  eV. These differences are consistent with

the ionic character of the salt which is demonstrated by comparing the separation in binding energy of the Pb  $5d_{5/2}$  and Te  $4d_{5/2}$  peaks in PbTe (20.01 eV) with the separation between these peaks in pure Pb and pure Te (21.48 eV). The difference of separations is 1.47 eV. The observed peak widths (FWHM) of the Pb 6s and the Te 5s in the pure elements are approximately a factor of 2 wider than peaks 2 and 3 in PbTe, possibly indicating a larger crystal field interaction for these bands in Pb and Te than in the partially ionic PbTe.

## V. CONCLUSIONS

We have presented the high-resolution XPS spectra of PbS, PbSe, and PbTe valence bands, assigned the peaks to bands in available calculated band structures, and compared the structure of each peak with theory. The agreement observed between theory and experiment is encouraging. Nevertheless, there are questions which remain to be answered before the full value of XPS valence-band spectra can be realized. We have assumed the one-electron transition model where the measured binding energy is equated to the one-electron orbital energy. This implies that all other one-electron orbitals remain frozen during photoemission. We have also assumed that the density of states  $\rho(E)$  generated from band-structure calculations corresponds to the one-electron orbital energy spectrum. The existence of possible deviations from the above model are recognized; however, they have to be defined and quantified before a more sophisticated model can be applied. Only by further experimental and theoretical study can the magnitude of the final state and relaxation effects in the photoemission process and the sensitivity of the theoretical band structure to an approximate exchange potential be taken into account.

## ACKNOWLEDGMENTS

One of us (L. L.) greatly appreciates a grant from the Max-Kade Foundation. We thank Professor G. Somorjai for giving us single-crystal PbS, PbSe, and PbTe.

\*Work performed under the auspices of the U.S. Atomic Energy Commission.

<sup>†</sup>On leave from University of Bonn, Germany.

<sup>‡</sup>In partial fulfillment of Ph.D.

<sup>1</sup>H. E. Swanson and R. K. Fuyat, *Circ. U.S. Natl. Bur. Stand.* **2**, 18 (1955).

<sup>2</sup>H. E. Swanson, N. T. Gilfrich, and G. M. Ugrinie, *Circ. U.S. Natl. Bur. Stand.* **5**, 39 (1955).

<sup>3</sup>N. R. Short, *Br. J. Appl. Phys.* **1**, 129 (1968).

<sup>4</sup>Pay June Lin and L. Kleinman, *Phys. Rev.* **142**, 478 (1966).

<sup>5</sup>Y. W. Tung and M. L. Cohen, *Phys. Rev.* **180**, 823 (1969).

<sup>6</sup>Y. W. Tung and M. L. Cohen (unpublished).

<sup>7</sup>F. Herman, R. L. Kortum, I. B. Outenburger, and J. P. Van Dyke, *J. Phys. (Paris)* **29**, C4-62 (1968).

<sup>8</sup>J. B. Conklin, Jr., L. E. Johnson, and G. W. Pratt, Jr., *Phys. Rev.* **137**, A1282 (1965).

<sup>9</sup>S. Rabii, *Phys. Rev.* **167**, 801 (1968); *Phys. Rev.* **173**, 918 (1968).

<sup>10</sup>C. S. Fadley and D. A. Shirley, in *Electronic Density of States*, Natl. Bur. Stand. Spec. Publ. No. 323 (U.S. GPO, Washington, D.C., 1971), p. 163.

<sup>11</sup>F. Herman, I. B. Outenburger, and J. P. Van Dyke, *Int. J. Quantum Chem. Symp.* **3**, 82 (1963).

<sup>12</sup>H. Overhof and U. Rössler, *Phys. Status Solidi* **37**, 691 (1970).

<sup>13</sup>M. Cardona and D. L. Greenaway, *Phys. Rev.* **133**, A1685 (1964).

<sup>14</sup>R. A. Pollak, L. Ley, S. Kowalczyk, D. A. Shirley, J. D. Joannopoulos, D. J. Chadi, and M. L. Cohen, *Phys. Rev. Lett.*

29, 1103 (1972).

<sup>15</sup>L. Ley, R. A. Pollak, S. Kowalczyk, and D. A. Shirley, Phys. Lett. A 41, 429 (1972).

<sup>16</sup>R. A. Pollak, S. Kowalczyk, L. Ley, and D. A. Shirley, Phys. Rev. Lett. 29, 274 (1972).

PHYSICAL REVIEW B

VOLUME 7, NUMBER 12

15 JUNE 1973

## Compositional Trends in the Optical Properties of Amorphous Lone-Pair Semiconductors\*<sup>†</sup>

Marc Kastner<sup>‡</sup> §

*Department of Physics, The University of Chicago, Chicago, Illinois 60637*

(Received 13 December 1972)

The pressure and temperature dependence of the refractive index and absorption edge have been measured for a group of amorphous semiconductors with average coordination number between two and four, all containing group-VI elements in twofold coordination (lone-pair semiconductors). Clear compositional trends are observed in the pressure dependence of the optical properties when these measurements are compared with the values for tetrahedral semiconductors. The chemical-bond approach is extended by the introduction of a new material parameter, the average bond-free solid angle (BFSA), in order to explain the large positive pressure coefficient of refractive index  $(\partial n/\partial P)_T$  observed for chalcogenide-rich materials and the small negative values observed for tetrahedral semiconductors. BFSA is the solid angle, associated with each atom, which is free of bond charge. When BFSA is large, atoms can move closer together under stress without compressing bonds. In this case local-field corrections cause positive  $(\partial n/\partial P)_T$ . When BFSA is small, local-field corrections are smaller because the charge density is more uniformly distributed. Strain results in bond compression which gives negative  $(\partial n/\partial P)_T$ . It is found that BFSA can also explain compositional trends in the pressure coefficient of the absorption edge as well as trends in apparently unrelated material properties such as melting temperature.

### I. INTRODUCTION

The chemical-bond approach to the origin of electronic states in solids has long been ignored by solid-state physicists since it cannot predict details of the electronic wave functions as can band theory. Chemical-bond arguments are capable, however, of predicting trends within classes of materials and therefore suggesting new materials with interesting properties. The chemical-bond approach is especially valuable in dealing with the properties of amorphous covalently bonded solids. Band theory is inadequate for these materials because they do not possess long-range order. On the other hand, their short-range order can be predicted or described by simple chemical-bond arguments.

Recently Phillips<sup>1</sup> has put the chemical-bond approach to solids on a firmer physical basis. He pointed out that chemical-bond arguments can be useful in describing properties which are determined by some average over all the valence electrons. In certain cases the low-frequency limit of the real part of the electronic dielectric constant is determined predominantly by the polarizability of the valence electrons. Phillips has used the dielectric constant to predict and understand trends within the class of  $A^N B^{8-N}$  crystals. He uses the dielectric constant to obtain a spectroscopic bond energy which is then separated into ionic and homo-

polar parts. A critical assumption in this analysis is that the homopolar part of the bond energy depends only on bond length  $a$  and goes as  $a^{-2.5}$ . Van Vechten<sup>2</sup> showed that this explains the negative pressure coefficient of refractive index  $(\partial n/\partial P)_T$  observed for  $A^N B^{8-N}$  tetrahedrally coordinated crystals.

It has been found,<sup>3</sup> however, that amorphous semiconductors containing large concentrations of group-VI elements in twofold coordination have positive  $(\partial n/\partial P)_T$ . It was pointed out that although the chemical bonding in these materials is very different from that in tetrahedral semiconductors [different enough, in fact, that they form a distinct class of materials—lone-pair (LP) semiconductors], nonetheless this difference in bonding cannot explain the different  $(\partial n/\partial P)_T$ . By invoking the Lorenz-Lorentz local-field correction, we can explain the positive values of  $(\partial n/\partial P)_T$  observed for materials very rich in group-VI elements. However, in order to understand the continuous change from positive to negative  $(\partial n/\partial P)_T$  as composition is varied in Se-Ge, we are forced to introduce in this work a new material parameter which is called the average bond-free solid angle (BFSA). In Sec. III BFSA is described, and its relation to the different chemical bonding in LP and tetrahedral materials is discussed.

The transitions in the values of  $(\partial n/\partial P)_T$  and the pressure coefficient of the absorption edge have not